Study of Runaway Electron Generation Process During Major Disruptions in JET.

V.V. Plyusnin 1), V. Riccardo 2), R. Jaspers 3), B. Alper 2), V.G. Kiptily 2), J. Mlynar 4),
S. Popovichev 2), E. de La Luna 5), P. Helander 2), F. Andersson 6)
and JET EFDA contributors.

1) Association Euratom-IST, Centro de Fusão Nuclear, Lisbon, Portugal
2) Euratom/UKAEA Fusion Association, Culham Science Centre, Abingdon, OX14 3DB, UK
3) Association Euratom-FOM, Nieuwegein, The Netherlands
4) Association Euratom - IPP.CR, Prague, Czech Republic
5) Association Euratom-CIEMAT, Madrid, Spain
6) VR-Euratom Association, Chalmers University of Technology, Gothenburg, Sweden

e-mail contact of main author: vladislav.plyusnin@cfn.ist.utl.pt

Abstract. The analysis of a large number of JET disruptions has provided further data on the trends of the disruption induced runaway process in large tokamaks. The role of primary runaway electrons generated at the thermal quench has been examined to assess their influence on secondary avalanching, which is recognized as a main source of large runaway currents created during disruptions. The tomographic reconstruction of the soft X-ray emission during the thermal quench has made possible the observation of the magnetic flux geometry evolution and the locating of the most probable zones for generation and confinement of the primary runaway electrons. Runaway currents have been found to increase with toroidal magnetic field and pre-disruption plasma current values. The average conversion efficiency is approximately 40-45% at a wide range of plasma currents. This agrees well with results of numerical simulations, which predict similar conversion rates at an assumed post-disruption plasma electron temperature of 10 eV. The experimental trends and numerical simulations show that runaway electrons might be an issue for ITER and therefore it remains prudent to develop mitigation methods, which suppress runaway generation.

1. Introduction

The generation of high-energy runaway electrons (REs) has been observed during numerous intentionally provoked and spontaneously occurring disruptions in JET [1-3]. Experimental data on disruptions and disruption generated REs in JET maintained from the beginning of JET operations [4] has been substantially extended during the recent experimental campaigns [2, 3, 5]. These studies provided further developments in understanding of important trends of runaway electron generation at disruptions in large tokamaks. Similarly to other large tokamaks [6], runaways have not been observed in JET below a certain threshold in toroidal magnetic field ($B_0 \leq 2$ T). A relatively high electron temperature ($Te>100$ eV) during disruption results in slow current quench and the absence of significant runaway generation. These latest results are in agreement with the earlier observations made in JET disruptions prior to the divertor installation [4], when the probability of REs generation in beryllium-bounded disruptions was significantly lower in comparison to that in carbon-bounded cases due to higher electron temperature immediately before the plasma current quench, i.e. carbon release during disruption caused much stronger cooling effect in comparison to beryllium. Very high electron density or strong MHD activity also caused the absence of REs at spontaneous disruptions in JET. However, a large number of spontaneous disruptions occurring at the different experimental conditions, namely, toroidal magnetic fields, plasma currents, triangularity and elongations caused a significant runaway process. Sometimes the runaway current tails reached more than 50% of the pre-disruptive plasma currents. A detailed evaluation of the experimental data and numerical modelling has allowed an assessment of the parameters and mutual dependence of two mechanisms responsible for

creation of runaway electrons during JET disruptions. These mechanisms are the primary (Dreicer) acceleration [7] and secondary avalanching [8, 9]. The results of numerical simulations and experimental data analysis show that disruption generated runaway electrons are the critical issue for future reactor-scale devices, like ITER [10], since the localized deposition of several Mega-Amperes of multi-MeV runaway electron current onto the components of the first wall can cause severe damage. It remains therefore prudent to develop mitigation techniques, which suppress runaway generation. Some results on the development of mitigation techniques, such as, massive gas puff, use of external magnetic error fields and auxiliary plasma heating, are presented in this paper.

2. Characteristics of Disruption Generated Runaway Electrons in JET.

Detailed analysis of intentional and spontaneously occurring disruptions has been carried out for further understanding of the trends of disruption induced runaway process. The reasons for spontaneous disruptions in JET were a consequence of the device operating near instability thresholds in safety factor, plasma pressure or plasma inductance in a wide range of toroidal magnetic field and plasma current values [1]. Intentional disruptions have been induced by programmed gas puff (neon and argon) to obtain long-lived runaway beam in order to increase the reliability of the measurement of parameters in REs. Another purpose of these experiments was to investigate several methods for the suppression or mitigation of the runaway generation at disruptions, such as, excitation of magnetic perturbations using external field coils, techniques that use massive helium gas puff and additional plasma heating by Low Hybrid Waves to decrease resistive electric fields. From the safety viewpoint, experiments on disruptions and runaways have been performed in the limiter configuration with low elongated plasmas. These configurations also provide more stable behaviour of runaway current carrying channel after disruptions. An example of a long-lived runaway beam generated during intentionally provoked disruption (pulse #63117, $I_{RAE} \sim 1$ MA, duration ~100 msec) together with an illustration of one of the highest conversion rate of plasma current into runaways (pulse #53790, $I_{RAE} \sim 1.3$ MA) are presented in Fig. 1(a, b). All characteristic features, which highlight the generation of the high-energy runaway electrons, including the current plateaux and simultaneous increases of the hard X-rays and neutron emissions, are presented. The evolution of these signals is compared to the contour plot of the soft X-ray emission measured during disruption by the horizontal set of detectors [11]. Intensive interaction of the beam of energetic runaway electrons with the plasma facing components in JET resulted in large heat loads, melting and sputtering of their covering material (Fig. 2).

Numerous theoretical studies (for example, [9]) predict that the avalanching growth of the secondary high-energy runaway electrons due to close electron-electron collisions between existing (primary) runaway electrons and thermal ones is the main source for large runaway currents observed in disruption experiments. The sequence of events preceding the current quench phase at disruption is well known and its detailed phenomenological description can be found elsewhere [1-3]. Loss of the plasma energy within a very short time due to strong perturbations results in a large increase of resistive electric fields enabling the creation of the high-energy primary REs. A modelling of the primary runaway process during disruption thermal quench in large tokamak (for example, [12]) has demonstrated that Dreicer acceleration provides a substantial number of runaway electrons with energies sufficient enough to enable the avalanching process. The parameters of primary REs and their mutual influence with the secondary process in JET have been assessed in a frame of the test particle model [13]. A set of equations ((1)-(3)) has been used for this modelling.
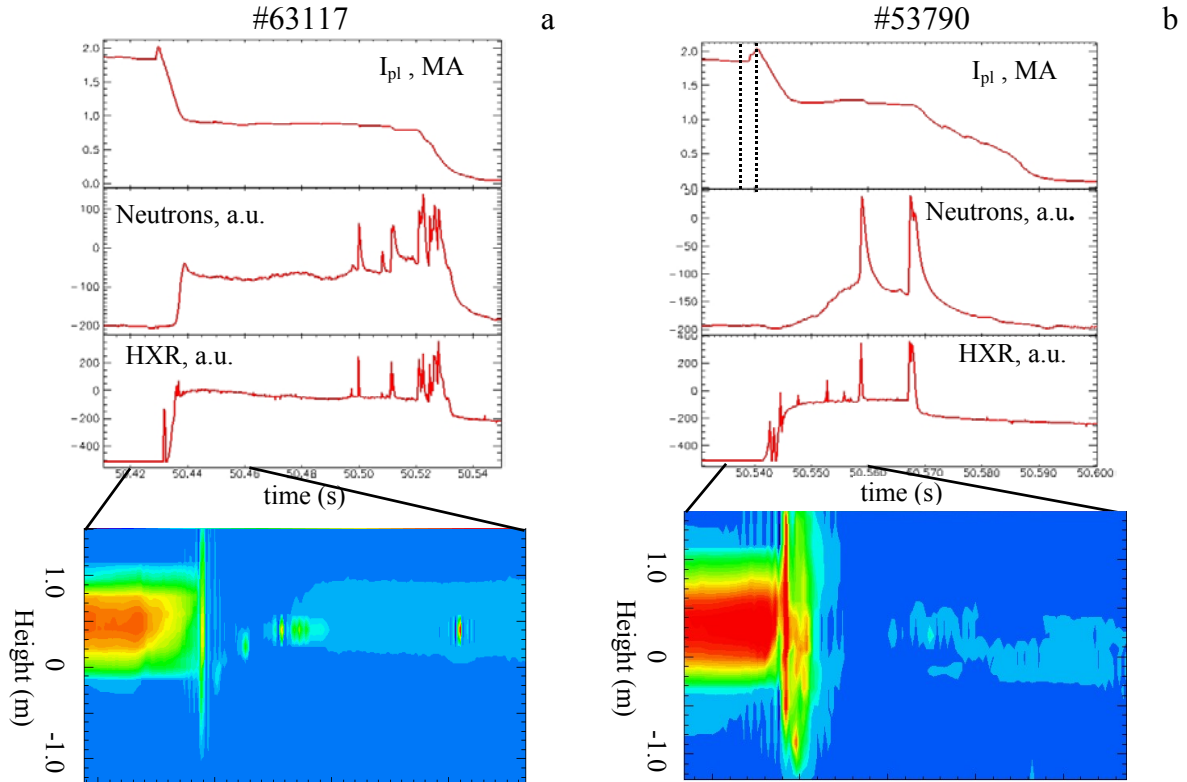
Fig. 1. Generation of runaway electrons at disruptions #63117 (a) and #53790 (b). Temporal evolutions of plasma currents, hard X-ray and photo-neutron emissions are compared to contour plot of the soft X-ray emissions measured by horizontal set of detectors in time ranges marked by lines. Vertical lines in chart (b) show time interval in which the soft X-ray tomography reconstruction has been performed (on Fig.5)

Disruption initiation   Interaction of runaway beam with wall   Sputtering of wall material and heat decay.
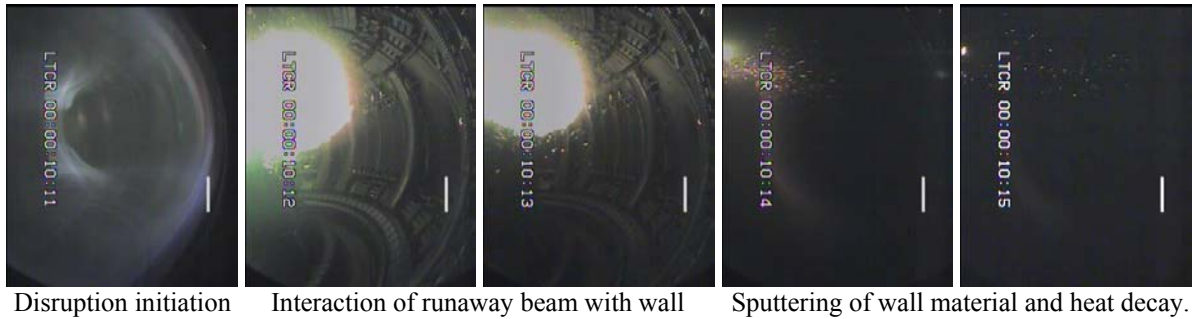
Fig. 2. Interaction of runaway beam with plasma facing components in JET during disruption #63117.

The initial conditions in this modelling have been inferred from the accessible experimental (plasma current, density, etc.) or, in some cases, reasonably assumed parameters (temperature, Z_{eff}, etc.) [14]. The dynamics of the runaway electrons, which experience the acceleration in the electric field (the first terms in right-hand side of equations (1)-(2)), collisions with the plasma particles (the second terms) and the sum of synchrotron radiation losses due to guiding centre motion and electron gyromotion (the third terms), has been simulated. Inclusion of the avalanching term into the equation for the runaway density evolution (Eq. (3)) made it possible to clarify the role of the avalanching process at the early stage of disruption. The evolution of electric filed in plasma has been modelled taking into account that plasma resistive current has been substituted by runaways and in assumption that plasma current decays exponentially during disruption. It was assumed that there were no losses of runaways.

$$\frac{dP_{||}}{dt} = \frac{e}{m_e c} E_{||} - \frac{e^4 n_e \ \ln \Lambda}{4\pi\varepsilon_0^2 m_e^2 c^3} \gamma(\gamma+\alpha)\frac{P_{||}}{P^3} - \frac{e^4 n_e \ \ln \Lambda}{4\pi\varepsilon_0^2 m_e^2 c^3}\frac{2B_0^2\varepsilon_0}{3m_e n_e \ \ln \Lambda}\left(\frac{m_e^2 c^2}{e^2 B_0^2 R_0^2} + \frac{P_\perp^2}{P^4}\right)\gamma^4\beta^3\frac{P_{||}}{P} \quad (1)$$

$$\frac{dP}{dt} = \frac{e}{m_e c} E_{||}\frac{P_{||}}{P} - \frac{e^4 n_e \ \ln \Lambda}{4\pi\varepsilon_0^2 m_e^2 c^3}\frac{\gamma^2}{P^2} - \frac{e^4 n_e \ \ln \Lambda}{4\pi\varepsilon_0^2 m_e^2 c^3}\frac{2B_0^2\varepsilon_0}{3m_e n_e \ \ln \Lambda}\left(\frac{m_e^2 c^2}{e^2 B_0^2 R_0^2} + \frac{P_\perp^2}{P^4}\right)\gamma^4\beta^3 \quad (2)$$

$$\frac{dn_{RA}}{dt} = \lambda_{RA} - \frac{n_{RA}}{\tau_R} + \frac{n_{RA}}{t_0} \quad (3)$$

Where $P_{||}$, $P_\perp$, P – are the parallel, perpendicular and total electron momenta normalized to $m_e c$, $\alpha = Z_{eff} + 1$, $\varepsilon = E_{||}/E_{DR}$, $E_{DR} = e^3 ln\Lambda n_e Z_{eff}/4\pi\varepsilon_0^2 T_e$, $E_{CR} = E_{DR}(T_e/m_e c^2)$, γ - relativistic factor, B_0 – toroidal magnetic field, R_0 – plasma major radius,

$$E_{||} = -\frac{L_{pl}}{2\pi R_0}\frac{dI_{pl}}{dt} = \eta_{pl} j_{pl}\left(1 - \frac{I_{RA}}{I_{pl}}\right)$$ - Evolution of the electric field,

$$t_0 = \frac{4\pi\varepsilon_0^2 m_e^2 c^3}{e^4 n_e}\sqrt{\frac{3}{\pi}}(Z_{eff}+5)\left(\frac{E_{||}}{E_{CR}}-1\right)^{-1}$$ - Secondary avalanching characteristic growth time,

$$\lambda_{RA} = C(Z_{eff})n_e \nu_e \varepsilon^{-3(Zeff+1)/16} \exp\left[-\frac{1}{4\varepsilon} - \sqrt{\frac{(Z_{eff}+1)}{\varepsilon}}\right]$$ - Runaway generation rate.
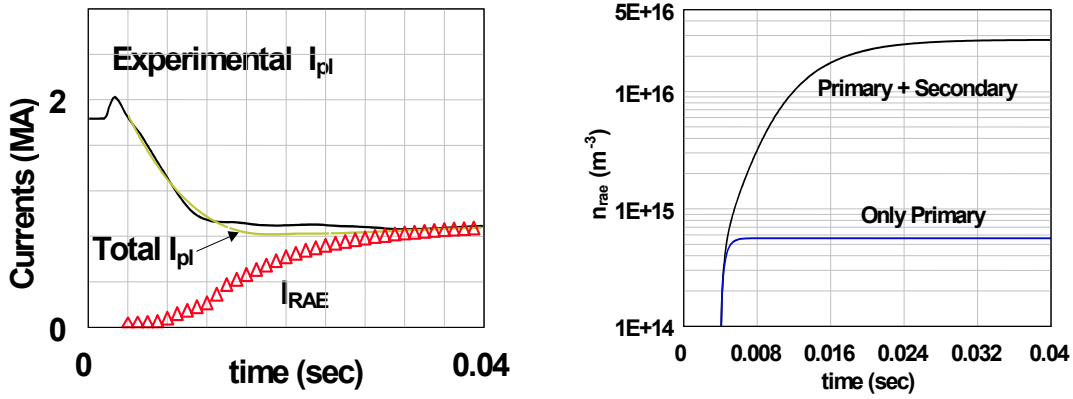

Fig. 3. Modelled evolution of runaway current and comparison of the measured plasma current to the calculated total current assuming exponential decay of the resistive plasma current with characteristic time 0.01 s (left chart). Calculated runaway electron density for primary only and for primary+avalanching mechanisms of runaway electron generation (right chart).
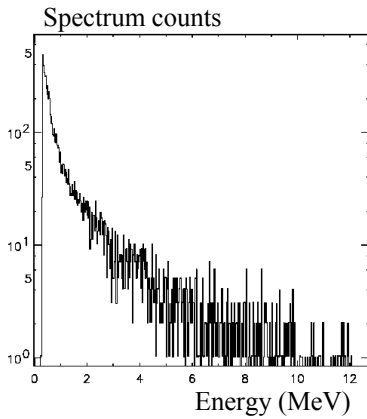

Fig. 4. Measured spectrum of photo-neutrons (#63117)

This modelling (Fig. 3) revealed a very close correspondence of calculated current evolution including runaways to the experimental evolution of the plasma current taking into account changes of the current-carrying channel cross-section (i.e. $r_{beam} = f(t)$), which are visible in soft X-rays (Fig. 1). The hard X-rays and photo-neutron production signals have been used to evaluate the energy of the runaway electrons, that interact with plasma facing components in JET. Neutron emission bursts (Fig. 1 (a,b)) are the direct evidence that runaway energies can be as high as 11 MeV if these neutrons are caused by Fe(γ,n)-reaction, or even higher than 19 MeV, if they are the result of ^{12}C(γ,n)-reaction. Modelling of the runaway process has demonstrated (also, for example, [2, 11]), that the distribution function of REs generated by the primary mechanism is expected to be close to monoenergetic with very high average kinetic

energy. The avalanching mechanism creates a distribution function of REs with exponential shape and substantially lower energy. Analysis of the recent data on the scattered photo-neutron emission spectra (Fig. 4) allowed establishing a low-energy bound on the runaway electron energy ($W_{RAE} \sim 8\text{-}10$ MeV). From the comparison of experimental data and results of numerical simulations one can conclude that the secondary avalanching process causes the dominating part of the disruption generated runaway current plateaus in JET. This consideration agrees well with numerical modelling performed either by Monte Carlo simulation of the drift kinetic equation for relativistic electrons in toroidal geometry using the ARENA code or by solving a nonlinear system of equations for the runaway density that exploits earlier, analytical results on runaway production [15,16].

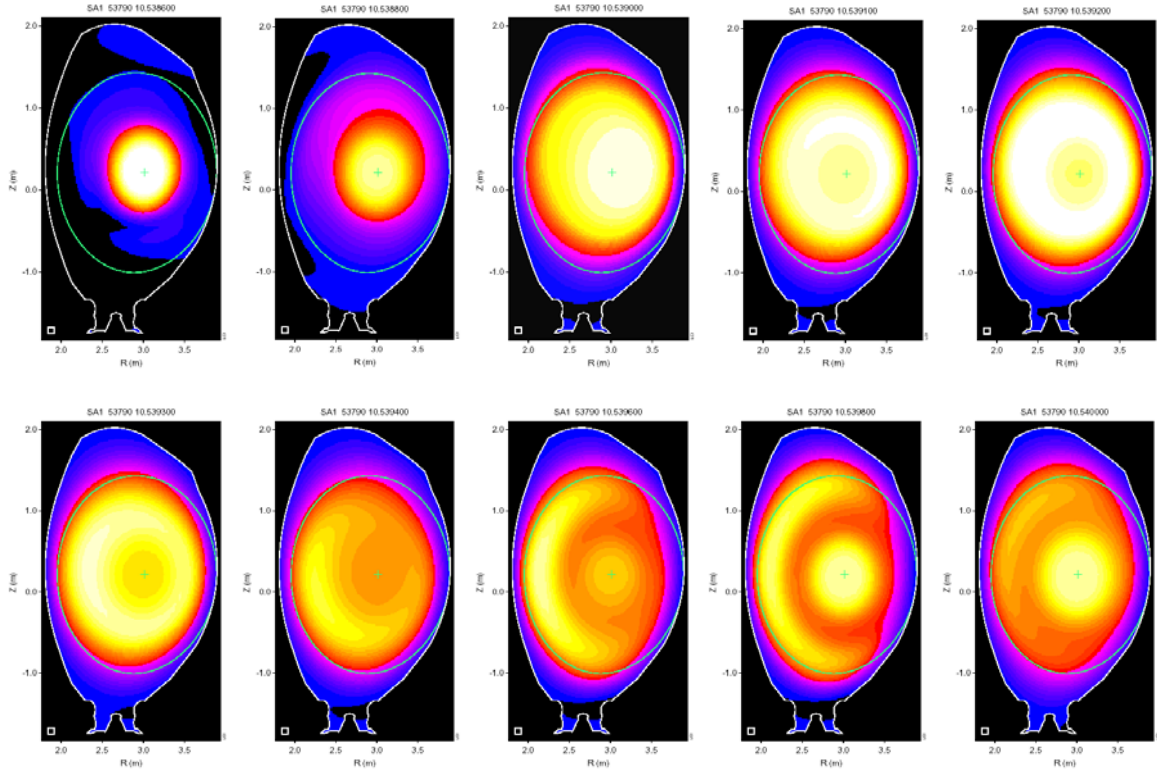## 3. Runaway Electrons and Evolution of Magnetic Configuration During Disruptions.

Fig. 5. Soft X-ray emission tomography reconstruction of the disruption #53790. Reconstructions have been made in time interval marked in Fig. 1(b) by vertical lines from $t_1 = 10.5386$ s up to $t_{last} = 10.54$ s.

Runaway generation has a continuous character during disruptions since a high electric field exists in the plasma during the thermal and current quenches. Energetic electrons have been detected immediately after the thermal quench when they produced a chain of soft X-ray emission spots and sometime large bursts of hard X-rays (Fig.1). The trajectories of soft-X ray spots obviously indicate that the thermal quench is a source of runaway electrons. However, REs are very sensitive to magnetic perturbations, which are very large during disruptions. Inevitable losses of REs limit the energy and total amount of REs before the current quench starts. The strong re-arrangement of the magnetic configuration during disruptions has been investigated in JET experiments. The tomographic reconstruction of the soft X-ray emission [17] during the thermal quench has made possible the observation of the magnetic flux geometry evolution and locating the most probable zones for generation and confinement of the primary runaway electrons. This reconstruction has been performed taking into account the fact that the energy isotropisation along the magnetic field lines is still

considerably faster than the evolution of the MHD modes even during thermal quench and, therefore, the assumption that the soft X-ray emission is constant on a magnetic flux surface remains valid throughout this stage. Figure 5 presents the temporally and spatially resolved evolution of the magnetic configuration in disruption #53790 on Fig. 1(b). The sequence of soft X-ray images provides a detailed view of the disruption reconnection event with expulsion of the plasma core and subsequent formation of confining magnetic structures. This information suggests that the formation of the nested magnetic surfaces structure in the plasma core confines an initial seed population of super-thermal or low energy runaway electrons, which are further accelerated. As the runaway electrons gain more energy at the current quench, the soft X-rays become a consequence of the interaction of the runaway beam with heavy impurity atoms [2], when it hits the surrounding surfaces of the device. A clear coincidence between the bursts of hard X-rays and neutron emissions and the appearance of the soft X-rays bursts, when runaway beam hits the wall, has been observed.

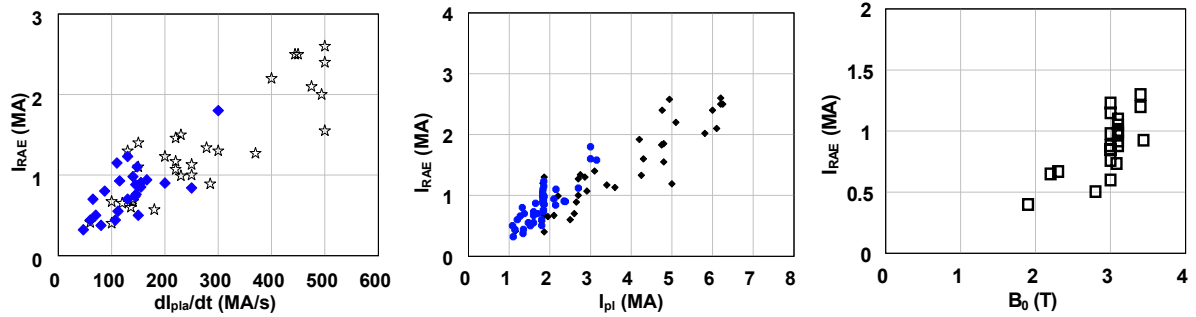## 4. Trends in Disruption Generated Runaway Electrons in JET.

Fig. 6. Dependencies of runaway current values on plasma current derivative (left chart) at the current quench stage prior (grey stars) and after (blue diamonds) divertor installation, on pre-disruptive plasma current values (central chart) and on the values of toroidal magnetic field (right chart) in experiments with pre-disruptive currents $I_{pl} = 1.8$-1.9 MA.

In this chapter we summarize the recent experimental data on disruption generated runaway electrons in JET ($I_{pl} \leq 3.5$ MA) with the addition of some data obtained at high-current disruptions prior to divertor installation in JET ($I_{pl} \leq 7$ MA) when 2-3 MA runaway current plateaus were obtained. The experimental data on disruption generated REs in JET demonstrates a fairly linear dependence of the runaway current on plasma current derivative and pre-disruptive plasma current values (Fig. 6 (a,b)). The average conversion efficiency of the plasma current into runaway current is approximately 42-45% for experiments carried out prior and after divertor installation in JET. This issue is in adequate agreement with the results of numerical simulations, which predict similar conversion rates at an assumed post-disruption average electron temperature of 10 eV [15, 16]. This modelling also predicts that at disruptions in ITER the current conversion efficiency could reach 60%. The increase of operational limits on toroidal magnetic field values obviously leads to improvement of the confinement of the runaway electrons and runaway current values, respectively (Fig. 6 (c)). A doubling of the toroidal magnetic field resulted in an increase of the photo-neutron production by two orders of magnitude. Summary trends of the data on runaways observed at disruptions prior and after divertor installation and the results of numerical modelling suggest that in disruptions, which might occur at the ITER nominal Q=10 parameters ([18]: I_{pl}=15 MA, n_e=10^{20} m^{-3}, MHD safety factor q_{95} =3) the generated runaway current could reach 10 MA in the MeV energy range.

5. Experiments on Suppression Techniques for Runaway Electrons in JET.

Since the intensive beams of energetic electrons generated at disruptions can lead to severe damaging of plasma facing components in reactor scale devices, several approaches to suppress runaway generation at disruptions have been studied in JET experiments. Magnetic field perturbations created by external field coils have been applied with the purpose of preventing runaway electron generation by enhancing the losses of runaways at an early stage during disruptions in JET. The current values in external field coils were limited in those experiments to 2 kA. Initial results show that this method had a noticeable effect only at intermediate toroidal field (i.e. preventing of runaway current plateau formation just above the threshold value) and actually had no effect at higher toroidal fields (Fig. 7(a)). Unlike the external magnetic fields perturbations, the massive helium gas puff into disruptive plasma efficiently prevented the runaway electron generation in JET. Analysis of the experimental data has shown that these disruptions have been characterised by relatively high electron temperature and a very fast increase of the plasma density, thus decreasing the runaway production rate. In the difference from argon and neon, the helium puff also provided substantially longer current quench stage with decreased plasma current derivative (Fig. 7(b)). Successfully being applied in JET, the method of intensive helium puff, however, requires further studies in order to assess the applicability of this feedback method for larger machines, since with the increase in the scale of devices the corresponding necessary gas quantity might be incompatible with experimental conditions. Attempts to mitigate runaway process with additional plasma heating (or current drive) at conditions of the density limit disruptions did not reveal any effect probably due to high plasma density at the boundary.
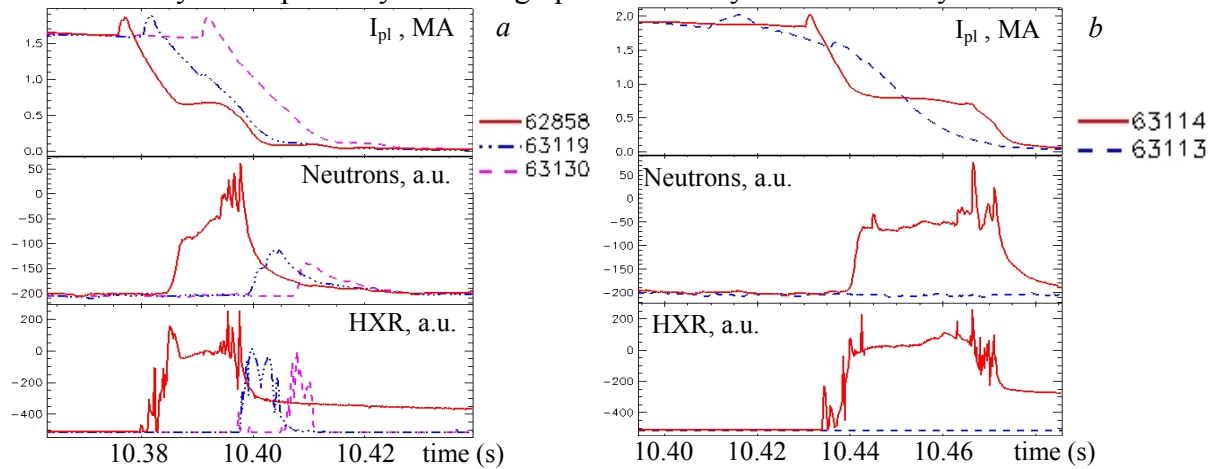

Fig. 7. Experiments on developments of runaway suppression techniques using magnetic perturbation excited by external coils, B_0= 2.6 T, (chart a) and using programmed helium puff (chart b). Temporal evolutions of plasma currents, hard X-ray (HXR) and photo-neutron emissions are compared for disruptions #62858-without external perturbations, disruptions #63119, #63130 – with external fields (a), and for #63113 with helium puff and for #63114 – without (chart b.)

6. Conclusions.

1. Despite strong perturbations, a significant amount of primary runaway electrons has been generated at the early stage of disruptions in JET. Runaway electrons with energies up to 2 MeV have been detected using soft X-ray and hard X-ray diagnostics.
2. Soft X-ray emission tomography allowed observation of the magnetic configuration evolution during a disruption. After fast expulsion of the hot plasma core, subsequent formation of the confining magnetic structures and creation of a narrow current

    carrying channel has been observed. Such a configuration provided the confinement of existing runaway electrons.

3. With the increase of size field and current in tokamak experiment the disruption generated runaway currents might be up to 60% of the pre-disruptive currents. At ITER nominal parameters the estimated runaway currents can reach 10 MA in the MeV-energy range. At these parameters runaway electrons will inevitably cause severe damage of the device if they are locally deposited onto the components of the first wall.

4. The experiments on the development of the methods for suppression or mitigation of runaway electron generation at disruptions have been carried out in JET. The use of externally applied magnetic field perturbations resulted in a noticeable effect only at medium values of toroidal magnetic fields and had no effect at higher toroidal fields. Efficient prevention of runaway generation at disruptions has been achieved by massive helium puff. Successfully being applied in JET, the method of intensive helium puff, however, requires further studies in order access the applicability of this feedback method to larger machines, since with the increase in the scale of devices the corresponding necessary gas quantity might be incompatible with experimental conditions.

7. Acknowledgements.

References.

[1] Wesson, J., Gill, R. D., Hugon, M. et al. Nuclear Fusion 29 (1989) 641
[2] Gill, R.D. et al. Nuclear Fusion 42(2002)1039;
[3] Riccardo, V., Plasma Phys. and Controlled Fusion, 45(2003) A269 -A284.
[4] Harris, G. R. Comparison of the current decay during carbon-bounded and beryllium-bounded disruptions in JET. JET preprint. (1990) JET-R(90)07
[5] Plyusnin, V. V. et al. In: Proceedings of the 30th EPS Conference on Contr. Fusion and Plasma Physics, St. Petersburg, 7-11 July 2003 ECA Vol. **27A**, P-2.94
[6] R.Yoshino, S. Tokuda. Nuclear Fusion 40(2000)1293
[7] Dreicer, H., Physical Review 115(1959)238
[8] Sokolov, Yu. A. JETP Letters 29(1979)218
[9] Rosenbluth, M. N. and Putvinski, S. V. Nuclear Fusion 37 (1997) 1355
[10] ITER Physics Basis, Nuclear Fusion 39 (1999) 2137-2638
[11] Alper, B. et al. Rev. Sci. Instrum. 68(1), January 1997, 778
[12] Plyusnin, V. V., et al. Plasma Phys. Control. Fusion **44** (2002) 2021–2031
[13] Esposito, B., et al. Phys Plasmas 6 (1999) 238-252
[14] White, D. G., et al. Physics of Plasmas, 7(2000)4052
[15] Helander, P., et al. Plasma Phys. Control. Fusion 44 (2002) B247–B262
[16] L.-G. Eriksson, P. Helander, F. Andersson, et al. Phys. Rev. Lett., to be published (2004)
[17] Ingesson, L.C. et al., Nucl. Fusion 38 (1998) 1675
[18] R. Aymar et al. Nuclear Fusion 41(2001)1301